Cooperative MEC-Enabled HAPS and UAV-RIS Assisted Task Offloading in ITS Systems

Insaf Rzig*† , Wael Jaafar†, Maha Jebalia*, and Sami Tabbane*
*MEDIATRON Laboratory, École Supérieure des Communications (Sup'Com), University of Carthage, Tunisia
†Department of Software and IT Engineering, École de technologie supérieure (ÉTS), University of Quebec, Canada
{insaf.rzig, maha.jebalia, sami.tabbane}@supcom.tn, wael.jaafar@etsmtl.ca

***Abstract*—Non-Terrestrial Networks (NTNs), comprising Unmanned Aerial Vehicles (UAVs) and High Altitude Platform Stations (HAPS) equipped with Mobile Edge Computing (MEC), offer promising solutions for network traffic and tasks offloading from ground users. To enhance the reliability and energy efficiency of such systems, Reconfigurable Intelligent Surfaces (RIS) can be deployed to control wireless signal propagation. In this context, we propose in this paper a novel MEC-enabled framework with HAPS and RIS-equipped UAVs (UAV-RISs) to optimize task offloading from ground users. Our objective is to minimize the tasks' average end-to-end (E2E) delay, under constraints of UAV and HAPS power capacity and E2E service delay threshold, through the optimization of task assignment and UAV-RIS phase-shift configuration. Given the NP-hardness of the problem, we decompose it into two subproblems. The first consists of optimizing the RIS phase shifts to minimize the RIS-assisted communication delay. The second tackles the task assignment problem using a Particle Swarm Optimization (PSO)-based approach, considering the RIS phase shifting solution previously developed. Through simulations, we validate the efficacy of our approach, which outperforms other benchmarks in terms of task average E2E delay and task offloading success rate.**

***Index Terms*—Intelligent Transportation Services, ITS, UAV, HAPS, MEC, RIS, NTN, PSO.**

I. Introduction

Future 6G wireless networks face escalating demands for expanded coverage, higher data rates, and stringent performance requirements, driven by the rapid proliferation of mobile devices and Internet-of-Things (IoT) applications such as Intelligent Transportation Services (ITS) [1], [2]. To effectively meet those demands, Mobile Edge Computing (MEC) has emerged as a crucial technology, decentralizing computation and storage resources closer to end-users, thus significantly reducing latency and resource constraints [3]. Nevertheless, terrestrial networks may be seen as inadequate due to inherent physical and geographical limitations, such as limited coverage in remote and hard-to-reach areas, prompting increased exploration of Non-Terrestrial Networks (NTNs). According to the Third Generation Partnership Project (3GPP), NTNs consist of aerial platforms including Unmanned Aerial Vehicles (UAVs), High Altitude Platform Stations (HAPS), and satellites [4]. These platforms offer enhanced coverage and robust connectivity, coupled with computational capabilities through integrated MEC functionalities, thereby significantly improving service delivery beyond traditional terrestrial reach [5]. Moreover, recent advancements in Reconfigurable Intelligent Surfaces (RISs), for dynamic control and manipulation of wireless propagation environments, promise substantial improvements in network energy efficiency [6]. Finally, integrating RIS within NTN is an emerging research direction that is still under investigation [7], [8].

Recently, several works have studied the integration of UAVs, MEC, and RIS, demonstrating substantial performance improvement when combined. Targeting to maximize the energy efficiency of RIS-assisted UAV-based Non-Orthogonal Multiple Access (NOMA) communication with ground users, the authors of [9] proposed a Dinkelbach-based iterative algorithm combined with block coordinate descent (BCD) to jointly optimize the facade-mounted RIS phase shifts, bit allocation, UAV transmit power, and UAV trajectory. In [10], the joint problem of RIS phase shifts configuration, UAV trajectory, and power allocation is investigated to minimize energy consumption and maximize overall energy efficiency. The authors in [11] investigated a RIS-assisted UAV-enabled MEC system aiming to improve system stability with reduced long-term energy consumption, through the joint optimization of computing resources, time slot allocation, transmit power, RIS phase shifting, and UAV trajectory. Although terrestrial RIS deployments face limitations in dynamic environments, RIS-equipped UAV (UAV-RIS) systems have gained traction due to their ability to maintain strong line-of-sight (LoS) links and dynamically enhance signal quality [12]. For instance, the authors of [13] deployed a UAV-RIS to minimize the total energy consumption through the joint optimization of UAV trajectory and amplification/phase shifting of the active UAV-RIS. In addition, the authors in [14] investigated the optimal deployment of UAV-RIS and resource allocation strategy to maximize reliability in Ultra Reliable Low Latency Communications (URLLC) systems, while ensuring fair user treatment.

Motivated by the recent advances in aerial platforms' communication capabilities and payload to support onboard MEC, such as UAVs and HAPS, and by developments in RIS technology, we propose here a novel and collaborative MEC-enabled HAPS and UAV-RIS framework that synergizes multiple UAV-RISs with MEC capabilities at both HAPS and UAV-RISs to enhance task offloading from ground users. The main contributions of this paper can be summarized as follows:

1) We formulate a joint optimization problem for task assignment and UAV-RIS phase shifting to minimize this framework's end-to-end (E2E) task offloading delay.
2) To handle the NP-hardness of the formulated problem,

979-8-3503-9281-4/25/$31.00 ©2025 IEEE

we decompose it into two subproblems, namely, RIS phase shifting and task assignment.

3) We derive a closed-form solution for RIS phase shifting using a semidefinite relaxation (SDR) approach. Then, a Particle Swarm Optimization (PSO) algorithm is used to solve the task assignment subproblem, considering the output of the RIS phase shift configuration.
4) Through simulations, we prove the superiority of our method, in terms of task average E2E delay and task offloading success rate, compared to other benchmarks.

The remainder of the paper is organized as follows. Section II describes the system model. Section III formulates the optimization problem and presents the proposed solution. In Section IV, simulation results are provided. Finally, the paper is concluded in Section V.

II. System Model

As illustrated in Fig. 1, the network consists of a multi-layer architecture integrating ground IoT User Devices (IUD), N UAVs hovering at a constant altitude H_n and covering non-overlapping areas, and a single HAPS floating quasi-stationary at an altitude of $H_0 = 20$ km and covering the whole region. Let the set $\mathcal{K} = \{1, 2, \ldots, K\}$ identify the K IUDs uniformly distributed in the area, while the set $\mathcal{N} = \{0, 1, 2, \ldots, N\}$ corresponds to the HAPS (index 0) and N UAV-RISs.

The coordinates of IUD k are identified by $\mathbf{q}_k = (x_k(t), y_k(t), 0)$, those of UAV-RIS n are $\mathbf{q}_n = (x_n, y_n, H_n)$ and similarly, the HAPS has coordinates $\mathbf{q}_0 = (x_0, y_0, H_0)$, with $t \in \mathcal{T} = \{0, 1, 2, \ldots, T\}$ refers to time slot t, assuming that time is discretized into time slots with each having duration τ seconds. In our system, each UAV-RIS n carries a passive RIS and one antenna (antenna is used for data reception or feedback transmission to an IUD). The RIS is characterized by M_n reflective elements, arranged in a uniform rectangular array (URA). It is also equipped with a microcontroller that dynamically adjusts the phase shifts of each reflective element. We define by $\mathbf{\Theta}_n(t) = \text{diag}\left(e^{j\theta_{n,1}(t)}, e^{j\theta_{n,2}(t)}, \ldots, e^{j\theta_{n,M_n}(t)}\right)$ the corresponding UAV-RIS phase shifting matrix, where $\theta_{n,i}(t) \in [0, 2\pi]$, $\forall i = 1, \ldots, M_n$. For the sake of simplicity, we represent the Euclidean distance between IUD k and UAV n as $d_{k,n} = \|\mathbf{q}_k - \mathbf{q}_n\|_2$, the distance between neighboring UAVs n and n' as $d_{n,n'} = \|\mathbf{q}_n - \mathbf{q}_{n'}\|_2$, and the distance between UAV n and the HAPS as $d_{n,0} = \|\mathbf{q}_n - \mathbf{q}_0\|_2$.

A. Channel Model

We assume that the channel state information (CSI) is perfectly known and that all communication channels experience quasi-static flat fading, i.e., remain constant within each communication. We also assume that the IUD, due to its limited power, cannot communicate directly with the HAPS. Hence, one of two communication modes can occur, namely 1) direct transmission from the IUD to its serving UAV (i.e., under its coverage), or 2) RIS-assisted communication between the IUD and a neighboring UAV/HAPS, via its serving UAV-RIS.

Fig. 1: System model.

1) Direct communication: The IUD communicates directly with its serving UAV, which is responsible for providing local computing to process the IUD's task. The channel coefficient between the IUD k and UAV n follows the Rician model, i.e.,

$$\mathrm{h}_{k,n} = \sqrt{\rho_0 d_{k,n}^{-\alpha_{k,n}}} \left(\sqrt{\frac{\beta_{k,n}}{1+\beta_{k,n}}} \mathrm{h}_{k,n}^{\mathrm{LoS}} + \sqrt{\frac{1}{1+\beta_{k,n}}} \mathrm{h}_{k,n}^{\mathrm{NLoS}} \right), \tag{1}$$

where ρ_0, $\alpha_{k,n}$ and $\beta_{k,n}$ are the average referenced channel power gain, the pathloss exponent, and the Rician factor, respectively. The LoS component is represented by $\mathrm{h}_{k,n}^{\mathrm{LoS}} = 1$ and $\mathrm{h}_{k,n}^{\mathrm{NLoS}}$ is the non-LoS (NLoS) component, modeled by the circularly symmetric complex Gaussian (CSCG) distribution with zero mean and unit variance [15]. Under the assumption that initiated communications by the IUDs are all orthogonal, the achievable data rate for this communication is given by $\mathrm{R}_{k,n} = B \log_2 \left(1 + P_k \|\mathrm{h}_{k,n}\|^2 / \sigma^2\right)$, where B represents the bandwidth allocated to a IUD-UAV communication, P_k is the transmission power of IUD k and σ^2 is the power of the additive white Gaussian noise (AWGN).

2) RIS-assisted communication: When an IUD k cannot be directly served by its covering UAV n due to limited resources, it may offload its task to a neighboring UAV n' or to the HAPS via its serving UAV's RIS. The corresponding channel vectors are denoted by $\mathbf{h}_{k,n} \in \mathbb{C}^{1 \times M_n}$ for the IUD–UAV-RIS link, $\mathbf{h}_{n,n'} \in \mathbb{C}^{M_n \times 1}$ for the UAV-RIS–neighbouring UAV link, and $\mathbf{h}_{n,0} \in \mathbb{C}^{M_n \times 1}$ for the UAV-RIS–HAPS link. We assume that communication links are dominated by Rician fading, hence, $\mathbf{h}_{k,n}$ can be expressed by

$$\mathbf{h}_{k,n} = \sqrt{\rho_0 d_{k,n}^{-\alpha_{k,n}}} \left(\sqrt{\frac{\beta_{k,n}}{1+\beta_{k,n}}} \mathbf{h}_{k,n}^{\mathrm{LoS}} + \sqrt{\frac{1}{1+\beta_{k,n}}} \mathbf{h}_{k,n}^{\mathrm{NLoS}} \right), \tag{2}$$

where $\mathbf{h}_{k,n}^{\text{LoS}} = \mathbf{a}_x(\Phi_{k,n}) \otimes \mathbf{a}_y(\Omega_{k,n})$ is the LoS component, where $\otimes$ denotes the Kronecker product, and the array response vectors are defined by

$$\mathbf{a}_x(\Phi_{k,n}) = \left[1, e^{-j\frac{2\pi}{\lambda}d_x\Phi_{k,n}}, \ldots, e^{-j\frac{2\pi}{\lambda}(M_{n,x}-1)d_x\Phi_{k,n}}\right]^T, \tag{3}$$

and

$$\mathbf{a}_y(\Omega_{k,n}) = \left[1, e^{-j\frac{2\pi}{\lambda}d_y\Omega_{k,n}}, \ldots, e^{-j\frac{2\pi}{\lambda}(M_{n,y}-1)d_y\Omega_{k,n}}\right]^T. \tag{4}$$

with λ is the carrier wavelength, d_x and d_y denote the distances of RIS elements along the X-axis and Y-axis, and $\Phi_{k,n} = \sin\theta_{k,n}\cos\varphi_{k,n} = \frac{y_n - y_k}{d_{k,n}}$, $\Omega_{k,n} = \sin\theta_{k,n}\sin\varphi_{k,n} = \frac{x_n - x_k}{d_{k,n}}$, are the vertical and horizontal Angle of Arrival (AoA) of the signal from IUD k to UAV-RIS n. Similarly, the channel vector $\mathbf{h}_{n,n'}$ can be written as

$$\mathbf{h}_{n,n'} = \sqrt{\rho_0 d_{n,n'}^{-\alpha_{n,n'}}}\left(\sqrt{\frac{\beta_{n,n'}}{1+\beta_{n,n'}}}\mathbf{h}_{n,n'}^{\text{LoS}} + \sqrt{\frac{1}{1+\beta_{n,n'}}}\mathbf{h}_{n,n'}^{\text{NLoS}}\right), \tag{5}$$

where $\alpha_{n,n'}$ and $\beta_{n,n'}$ are the path-loss exponent and the Rician factor, respectively. $\mathbf{h}_{n,n'}^{\text{LoS}} = \mathbf{a}_x(\Phi_{n,n'}) \otimes \mathbf{a}_y(\Omega_{n,n'})$, $\Phi_{n,n'} = \sin\theta_{n,n'}\cos\varphi_{n,n'} = \frac{(H_n - H_{n'})(y_n - y_{n'})}{d_{n,n'}d'_{n,n'}}$, and $\Omega_{n,n'} = \sin\theta_{n,n'}\sin\varphi_{n,n'} = \frac{(H_n - H_{n'})(x_n - x_{n'})}{d_{n,n'}d'_{n,n'}}$, with $d'_{n,n'} = \sqrt{(x_n - x_{n'})^2 + (y_n - y_{n'})^2}$ is the horizontal 2D distance. Consequently, using eq.(5), channel vector $\mathbf{h}_{n,0} = \mathbf{h}_{n,n'}$ where we set $n' = 0$.

We define the received signal-to-noise ratio (SNR) at the neighbouring UAV n or HAPS as $\psi_{k,n,n'}$, expressed by $\psi_{k,n,n'} = P_k \left\|(\mathbf{h}_{n,n'})^H \mathbf{\Theta}_{n,k}\mathbf{h}_{k,n}\right\|^2/\sigma^2$, and the data rate as $\mathrm{R}_{k,n,n'}^{\text{RIS}} = B\log_2(1+\psi_{k,n,n'})$.

B. Task Completion Delay Analysis

Each IUD task request can be generated at a given time slot t, and is characterized by the tuple $\varphi_k = \{S_k, C_k, T_k^{\max}\}$, where S_k denotes the input data size, C_k represents the number of CPU cycles required per bit, and $T_k^{\max}$ is the maximum tolerable delay for completing the task. We define a binary indicator variable $\chi_{k,n}$, which is equal to 1 if IUD k is assigned to MEC node n, with $n \in \mathcal{N}$, and 0 otherwise. We assume that both the UAVs and the HAPS follow a first-come, first-served queue management policy. Hence, the E2E delay of IUD task φ_k consists of three components, namely, communication delay, computation delay, and queueing delay[1].

1) Communication delay: When an IUD task is assigned to its serving UAV n, then the MEC mode is activated for local processing. Otherwise, i.e., the task is assigned to HAPS or another neighbouring UAV, the RIS mode is enabled at the serving UAV-RIS to forward the task φ_k to the assigned MEC node (UAV or HAPS). The uplink transmission delay can then be expressed by

$$D_{k,n}^{\text{up}} = \begin{cases} S_k/\mathrm{R}_{k,n}, & \text{if } \varphi_k \text{ assigned to its serving UAV } n \text{ (Direct)}, \\ S_k/\mathrm{R}_{k,n',n}^{\text{RIS}}, & \text{if } \varphi_k \text{ assigned to non-serving UAV } n \text{ (assisted by serving UAV-RIS } n'). \end{cases} \tag{6}$$

2) Computation Delay: The computation delay needed to complete task φ_k at any given MEC node depends on the CPU frequency f_n of its MEC server. It can be expressed as

$$D_{k,n}^{\text{comp}} = S_k C_k/f_n, \forall n \in \mathcal{N}. \tag{7}$$

Subsequently, the energy consumed by MEC node n is

$$E_{k,n}^{\text{comp}} = \kappa_n (f_n)^3 D_{k,n}^{\text{comp}}, \forall n \in \mathcal{N}, \tag{8}$$

where κ_n is the switched capacitance of the MEC server's chip architecture.

3) Queuing Delay: Similarly to [16], the queuing delay experienced by task φ_k in MEC node n can be given by

$$D_{k,n}^{\text{que}} = \sum_{i \in \mathcal{Q}_{k,n}} D_{i,n}^{\text{comp}}, \tag{9}$$

where $\mathcal{Q}_{k,n}$ is the set of tasks queued at node n prior to φ_k. Based on the above expressions, the E2E task completion delay of φ_k is expressed by

$$D_{k,n}^{\text{E2E}} = D_{k,n}^{\text{up}} + D_{k,n}^{\text{comp}} + D_{k,n}^{\text{que}}, \forall n \in \mathcal{N}, k \in \mathcal{K}. \tag{10}$$

III. Problem Formulation and Proposed Solution

A. Problem Formulation

Our objective is to minimize the E2E task completion delay by jointly optimizing task assignment decisions $\boldsymbol{\chi} \triangleq \{\chi_{k,n} \,|\, \forall n \in \mathcal{N}, k \in \mathcal{K}\}$ and RIS phase shift configurations $\mathbf{\Phi} \triangleq \{\theta_{n,i}(t) \,|\, \forall n \in \mathcal{N}, \forall i = 1, \ldots, M_n, \forall t \in \mathcal{T}\}$. The resulting problem can be formulated as follows:

$$\min_{\boldsymbol{\chi}, \mathbf{\Phi}} \quad \frac{1}{K}\sum_{k=1}^{K}\sum_{n=0}^{N} D_{k,n}^{\text{E2E}} \tag{P}$$

$$\text{s.t.} \quad D_{k,n}^{\text{E2E}} \le T_k^{\max}, \quad \forall k \in \mathcal{K}, n \in \mathcal{N}, \tag{P-a}$$

$$\sum_{k=1}^{K} E_{k,n}^{\text{comp}} \le E_n^{\text{cp,max}}, \quad \forall n \in \mathcal{N}, \tag{P-b}$$

$$\sum_{n=0}^{N} \chi_{k,n} \le 1, \quad \forall k \in \mathcal{K}, \tag{P-c}$$

$$\chi_{k,n} \in \{0,1\}, \quad \forall n \in \mathcal{N}, \forall k \in \mathcal{K}, \tag{P-d}$$

$$\theta_{n,i}(t) \in [0, 2\pi], \quad \forall n \in \mathcal{N}, i \in 1, \ldots, M_n, \tag{P-e}$$

(P-a) limits the total delay of task φ_k to its maximum threshold $T_k^{\max}$, while (P-b) restricts the processing energy at MEC node n to its maximum energy $E_n^{\text{cp,max}}$. (P-c) ensures that each IUD is assigned to at most one MEC node, and (P-d) enforces the binary nature of $\chi_{k,n}$. Finally, (P-e) limits the range of RIS phase shifts to $[0, 2\pi]$. Solving (P) is challenging due to the interaction among variables in the objective function and

[1]We assume here that the task outcome feedback time and energy to the IUD are negligible, and thus are ignored in the next calculations.

constraints. To make it tractable, we split it into two sub-problems, namely, UAV-RIS phase shift design and IUD task assignment, and solve them separately. Then, we combine the obtained solutions to develop the global solution to (P).

B. UAV-RIS Phase Shifting Optimization

Due to the non-convexity of (P-e), the resolution of (P) to find $\mathbf{\Phi}$ becomes challenging. We first present a proposition for the design of a phase shift for the dedicated communication between IUD k and its assigned UAV n via UAV-RIS n'.

Proposition 1: The optimal phase shifts for the RIS when assisting the transmission of task φ_k can be determined by solving the following problem:

$$\mathbf{\Theta}^*_{n',k} = \arg\max_{\boldsymbol{\theta}_{n',k}} \left|\mathbf{h}^H_{n,n'}\mathbf{\Theta}_{n',k}\mathbf{h}_{k,n'}\right|^2, \text{s.t.}\theta_{n',k,i} \in [0, 2\pi],\ \forall i, \tag{P1}$$

where $\mathbf{\Theta}_{n',k} = \text{diag}(e^{j\theta_{n',k,1}}, \ldots, e^{j\theta_{n',k,M_{n'}}})$, and $\theta_{n',k,i}$ is the phase shift of element i of UAV-RIS n' to forward φ_k.

Proof 1: Minimizing the objective function in (P) suggests minimizing the communication delay $D^{\text{up}}_{k,n}$, which is related to $\text{R}^{\text{RIS}}_{k,n',n}$ in eq.(6). Clearly, $\text{R}^{\text{RIS}}_{k,n',n}$ is an increasing function with $\left|\mathbf{h}^H_{n,n'}\mathbf{\Theta}_{n',k}\mathbf{h}_{k,n'}\right|^2$ for $k \in \mathcal{K}, n' \neq n, n' \in \mathcal{N} \setminus \{0\}$. Moreover, $\left|\mathbf{h}^H_{n,n'}\mathbf{\Theta}_{n',k}\mathbf{h}_{k,n'}\right|^2$ depends solely on the variable $\mathbf{\Theta}_{n',k}$. Hence, minimizing the objective of (P) by optimizing $\mathbf{\Phi}$ is equivalent to maximizing $\left|\mathbf{h}^H_{n,n'}\mathbf{\Theta}_{n',k}\mathbf{h}_{k,n'}\right|^2$ through the optimization of $\mathbf{\Theta}_{n',k}$.

According to Proposition 1, we can solve (P1) to obtain the optimal phase shifts of UAV-RIS n'-assisted communication between IUD k and UAV n. Let $v_{n',k,i} = e^{j\theta_{n',k,i}}$, where $|v_{n',k,i}|^2 = 1$, and $\phi_{n',k} = \text{diag}(\mathbf{h}^H_{n,n'})\mathbf{h}_{k,n'}$ and $\mathbf{v}_{n',k} = [v_{n',k,i}, \ldots, v_{n',k,M_n}]^H$. Hence, $\left|\mathbf{h}^H_{n,n'}\mathbf{\Theta}_{n',k}\mathbf{h}_{k,n'}\right|^2$ can be rewritten as $|\mathbf{v}_{n',k}\phi_{n',k}|^2 = \mathbf{v}^H_{n',k}\phi_{n',k}\phi^H_{n',k}\mathbf{v}_{n',k}$, and (P1) is reformulated as

$$\max_{\mathbf{v}_{n',k}} \mathbf{v}^H_{n',k}\phi_{n',k}\phi^H_{n',k}\mathbf{v}_{n',k}, \quad \text{s.t.}\,|v_{n',k,i}|^2 = 1, \forall i. \tag{P1'}$$

It can be observed that (P1') is non-convex and it is difficult to solve it directly, so we define an auxiliary variable $\mathbf{X}_{n',k} = \phi^H_{n',k}\phi_{n',k}$. Based on this, $\mathbf{v}^H_{n',k}\mathbf{X}_{n',k}\mathbf{v}_{n',k} = \text{Tr}(\mathbf{X}_{n',k}\mathbf{v}_{n',k}\mathbf{v}^H_{n',k})$. Consequently, let $\mathbf{V}_{n',k} = \mathbf{v}^H_{n',k}\mathbf{v}_{n',k}$, where $\mathbf{V}_{n',k} \succeq 0$ and $\text{rank}(\mathbf{V}_{n',k}) = 1$. Thus, (P1') can be reformulated as follows

$$\max_{\{\mathbf{V}_{n',k}\}} \quad \text{Tr}(\mathbf{X}_{n',k}\mathbf{V}_{n',k}) \tag{P1"}$$

$$\text{s.t.} \quad \mathbf{V}_{n',k} \succeq 0, \tag{P1"-a}$$

$$[\mathbf{V}_{n',k}]_{i,i} = 1, \quad \forall i = 1, \ldots, M_{n'}, \tag{P1"-b}$$

$$\text{rank}(\mathbf{V}_{n',k}) = 1. \tag{P1"-c}$$

where $[\mathbf{V}_{n',k}]_{i,i}$ is a diagonal element of matrix $\mathbf{V}_{n',k}$. According to the SDR method, we relax the rank-1 constraint (P1"-c) in the problem (P1"), and then use CVX toolbox to obtain the $(\mathbf{V}_{n',k})$.Since we relax the rank-1 constraint, the resulting matrix $\mathbf{V}_{n'k}$ may not satisfy $\text{rank}(\mathbf{V}_{n',k}) = 1$. However, we can recover a rank-1 solution and obtain $\mathbf{v}^*_{n',k}$ by applying the methods in [17].

C. IUD Task Assignment Optimization

Assuming that the UAV-RISs phase-shift configurations are pre-set, then (P) reduces to task assignment, written by

$$\min_{\boldsymbol{\chi}} \quad \frac{1}{K}\sum_{k=1}^{K}\sum_{n=0}^{N} D^{\text{E2E}}_{k,n}, \text{ s.t. (P-a)–(P-d).} \tag{P2}$$

Although (P2) is formulated as an integer linear program (ILP), traditional solvers, such as branch-and-bound, typically do not scale well and lack the real-time adaptability required in dynamic environments. To overcome these limitations, we adopt a PSO-based approach. PSO is a metaheuristic that efficiently navigates large combinatorial search spaces with moderate computational effort. Unlike genetic algorithms, PSO does not require the additional overhead of crossover, encoding, or decoding operations. Moreover, its inherent stochasticity promotes robust exploration of the solution space, enabling it to quickly identify high-quality near-optimal solutions even in rapidly changing scenarios [18].

Our PSO-based approach begins by generating random particle positions within the search space. Each particle j is represented by a matrix $\mathbf{Z}_j$ of size $K \times N$, where $\mathbf{Z}_j$ encodes a potential assignment between K IUDs and N UAVs. During each iteration δ, particle j updates its position using its personal best ($pbest_j$) and the global best ($gbest$) values, as determined by the fitness function calculated using the objective function in (P2). It is important to note that this calculation calls for the RIS phase-shift configurations, which are obtained through the solution to (P1"). The velocity updating for each particle is given by

$$\mathbf{W}_j{}^{\delta+1} = w\mathbf{W}_j{}^{\delta} + c_1 r_1 \left(\text{pbest}_\text{j} - \mathbf{Z}_j{}^{\delta}\right) + c_2 r_2 \left(\text{gbest} - \mathbf{Z}_\text{j}{}^{\delta}\right), \tag{13}$$

where w is the inertia weight, (c_1, c_2) represent the cognitive and social acceleration factors, respectively, while (r_1, r_2) are random values uniformly sampled from the interval $[0, 1]$. Subsequently, the particle updates its position by

$$\mathbf{Z}_j{}^{\delta+1} = \mathbf{Z}_j{}^{\delta} + \mathbf{W}_j{}^{\delta+1}. \tag{14}$$

This allows particles to traverse the search space while balancing the exploration of new regions with the exploitation of known optima. The steps of our global approach are summarized in Algorithm 1.

IV. Simulation Results

For our simulations, we consider a network deployed in an urban area with high-rise buildings, consisting of $K = 100$ IUDs, two MEC-equipped UAV-RISs ($N = 2$) and one MEC-equipped HAPS, observed during time $T = 300$ sec. The locations of the UAV-RISs are defined as $\mathbf{q}_1 = (500, 1000, 100)$ meters, $\mathbf{q}_2 = (1500, 1000, 120)$ meters, while the HAPS is located at $\mathbf{q}_0 = (1000, 1500, 20000)$ meters. The pathloss exponents are given by $\alpha_{k,n}$ = 2.5, $\alpha_{n,n'}$ = 2.8, and $\alpha_{n,0}$

Algorithm 1 Proposed Solution

Input: N, K, φ_k, $\mathbf{h}_{k,n}, \mathbf{h}_{n,n'}$, max. iter. $I_{\max}$.
Output: Task assignment policy $\boldsymbol{\chi}^*$
for particle j **in** swarm **do**
  Initialize position $\mathbf{Z}_j$ and velocity $\mathbf{W}_j$
  Solve (P1") to obtain optimal phase shifts $\boldsymbol{\Phi}^*$ for $\mathbf{Z}_j$.
  Evaluate fitness function $f(\mathbf{Z}_j)$ and initialize $pbest_j$
end for
for $\delta \leftarrow 1$ **to** $I_{\max}$ **do**
  for each particle j **do**
    Update velocity $\mathbf{W}_j^\delta$ using eq.(13)
    Update position $\mathbf{Z}_j^\delta$ using eq.(14)
    if $\mathbf{Z}_j^\delta$ violates a constraint from (P2-a)-(P2-d) **then**
      Apply repair mechanism to fix $\mathbf{Z}_j^\delta$
    end if
    Obtain optimal phase shifts $\boldsymbol{\Phi}^*$ for $\mathbf{Z}_j^\delta$.
    Evaluate fitness function $f(\mathbf{Z}_j^\delta)$ incorporating $\boldsymbol{\Phi}^*$.
    if $f(\mathbf{Z}_j^\delta) < f(pbest_j)$ **then**
      Update personal best $pbest_j \leftarrow \mathbf{Z}_j^\delta$
    end if
  end for
  if $f(\mathbf{Z}_j^\delta) < f(gbest)$ **then**
    Update global best $gbest \leftarrow \mathbf{Z}_j^\delta$
  end if
end for
Return $\boldsymbol{\chi}^*$.

= 2. Moreover, the Rician factors are uniformly set to $\beta_{k,n} = \beta_{n,n'} = 10$ dB, $\forall k \in \mathcal{K}$, $\forall (n, n') \in \mathcal{N}^2$. The bandwidth for communications initiated by the IUDs is $B = 1$ MHz. The noise power is $\sigma^2 = -100$ dBm, while the transmit powers of the IUD is $P_k \in [20, 23]$ dBm, $\forall k \in \mathcal{K}$ [19]. Unless stated otherwise, we assume the same number of reflective elements $M = M_n = 32$, $\forall n = 1, \ldots, N$. Moreover, a task φ_k is characterized by $S_k \in [0.15, 0.45]$ MegaBytes (MB), $C_k \in [800, 1000]$ cycles per bit, and $T_k^{\max} \in [200, 600]$ milliseconds (ms) [5]. We assume that the computation resources at the HAPS and UAVs are $f_0 = 20$ GHz and $f_1 = f_2 = 10$ GHz, respectively. For energy computation, we use $\kappa = 10^{-28}$, $E_0^{\text{cp,max}} = 50$ KiloJoules (KJ), and $E_n^{\text{cp,max}} = 1$ KJ, $n = 1, 2$.

We evaluate the performance of our approach, in terms of average E2E delay and success rate, using Monte-Carlo simulations, and compare them to those of benchmarks:

1) *Terrestrial-RIS (T-RIS):* Inspired by [9], we adapt our method to solve a similar problem to (P), but where RISs are located on building facades rather than on UAVs.
2) *Without RIS (Wo-RIS):* We adapt our approach to solve a similar problem where RISs are unused by the network.
3) *Local UAV-MEC:* IUD tasks are offloaded exclusively to the UAV connecting them.

Fig. 2 presents the average E2E delay as a function of the number of PSO iterations, for different values of K and M. Our method converges fast for any K and M (2 to 5 iterations). When K increases, the average E2E delay degrades. This is expected since more IUDs are generating and offloading more tasks, thus impacting the communication and queuing delays at UAVs and HAPS. Nevertheless, when the number of reflective elements M raises from 32 to 128, we notice a significant improvement in the average E2E delay. Indeed, the use of larger RIS favors faster communications and more offloading to beyond serving UAV (i.e., to HAPS and other UAV). The consistent convergence speed across all configurations demonstrates the algorithm's scalability and ability to identify near-optimal solutions for the joint optimization problem.

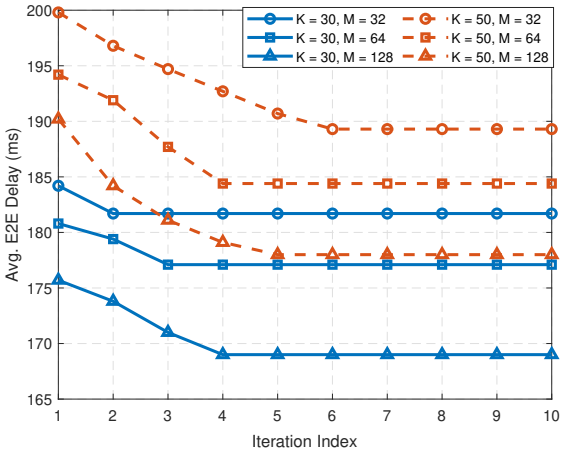

Fig. 2: Convergence of the proposed approach.

In Fig. 3, we analyze the impact of the number of IUDs K on the average E2E delay and success rate. As K grows from 30 to 100, the delay increases across all schemes due to higher communication and queuing for the additional generated tasks. Nevertheless, our solution consistently outperforms the benchmarks as it strategically assigns tasks between all MEC nodes. For instance, for $K = 100$, our method achieves an average E2E delay of 220 ms, satisfying 64% of the tasks, while the T-RIS ranks second. The latter's reliance on terrestrial RIS suffers from higher NLoS. Local-UAV-MEC maintains a stable delay but cannot handle more than 10% of tasks. Finally, Wo-RIS performs the worst since it doesn't use RIS.

Fig. 4 depicts the temporal evolution of task handling and residual energy along a given mission, when using our method. The top graph shows that while early tasks are mostly satisfied, a sharp increase in task arrivals around 134-155 seconds results in a rise in task failures. The bottom graph indicates that UAV 1 is overused initially, thus experiencing rapid energy depletion, nearing exhaustion by 101 sec, whereas UAV 2 and the HAPS maintain higher energy levels throughout the mission. This reflects the strategic early use of UAV 1, followed by load redistribution to UAV 2 and the HAPS to maintain service continuity as demand increases.

Fig. 5 studies the impacts of M, N and f_n on the E2E delay, using our method. When f_n increases, the E2E delay significantly improves for any M and N. When M is higher, the communication quality improves, thus reducing the E2E

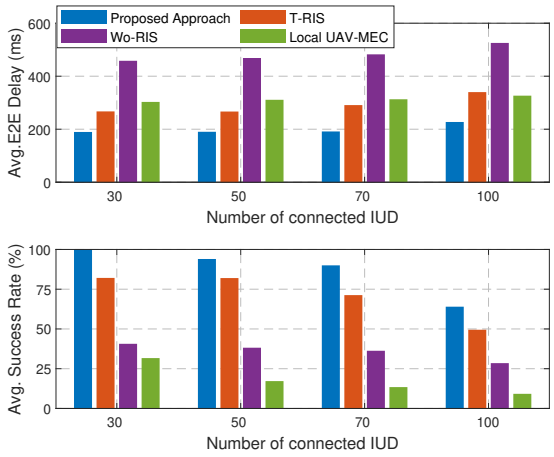

Fig. 3: Impact of number of connected IUDs.

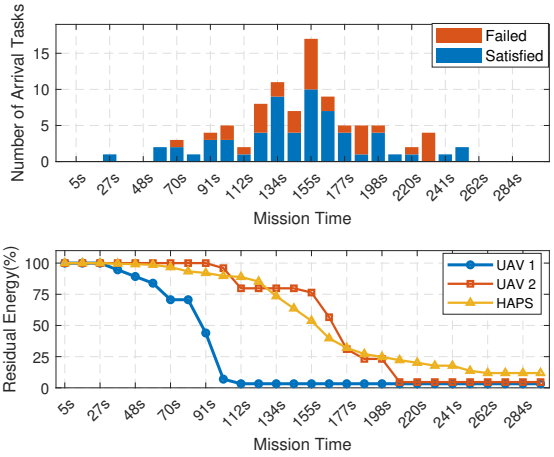

Fig. 4: Mission timeline analysis.

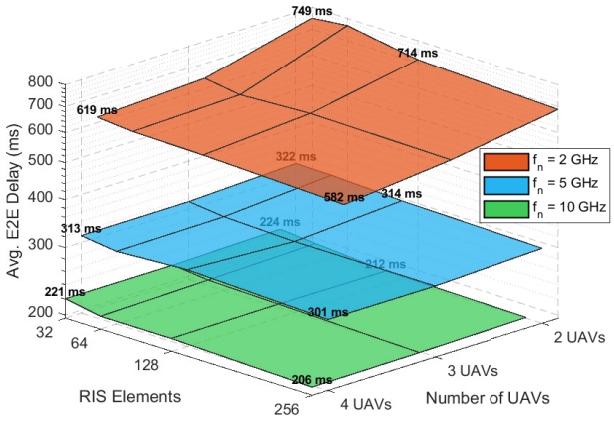

Fig. 5: Impact of number of RIS elements M, number of UAVs N, and UAV computing capacity f_n. (K = 100, f_0 = 20 GHz)

delay. However, it saturates at $M = 128$, suggesting the latter as the maximal M. Deploying more UAVs, i.e., higher N, enables effective load distribution and spatial coverage, with higher gains achieved when f_n is low.

V. Conclusion

In this paper, we introduced a novel cooperative approach for task offloading from IUDs to a heterogeneous MEC-equipped HAPS and UAV-RISs platform. By leveraging the flexibility of UAV-RISs and available MEC power, the proposed method effectively minimized E2E task completion delay while satisfying the delay QoS. Through simulations, we demonstrated the superiority of our approach over benchmarks in terms of E2E delay and success rate. Finally, the parametric study provides insights into the efficient configuration of HAPS/UAV-RIS-assisted task offloading in future networks.

References

[1] S. Dang *et al.*, "What should 6G be?" *Nature Electron.*, vol. 3, no. 1, pp. 20–29, 2020.

[2] W. Jaafar and H. Yanikomeroglu, "HAPS-ITS: Enabling future ITS services in trans-continental highways," *IEEE Commun. Mag.*, vol. 60, no. 10, pp. 80–86, Oct. 2022.

[3] Y. Mao *et al.*, "A survey on mobile edge computing: The communication perspective," *IEEE Commun. Surv. Tuts.*, vol. 19, no. 4, pp. 2322–2358, 2017.

[4] X. Cao *et al.*, "Airborne communication networks: A survey," *IEEE J. Sel. Ar. Commun.*, vol. 36, no. 9, pp. 1907–1926, 2018.

[5] I. Rzig *et al.*, "Dependency-aware task offloading in cooperative UAV-HAPS-assisted vehicular networks," in *Proc. Int. Wireless Commun. Mob. Comput.*, 2024, pp. 1541–1546.

[6] C. Liaskos *et al.*, "A new wireless communication paradigm through software-controlled metasurfaces," *IEEE Commun. Mag.*, vol. 56, no. 9, pp. 162–169, 2018.

[7] S. Alfattani *et al.*, "Aerial platforms with reconfigurable smart surfaces for 5G and beyond," *IEEE Commun. Mag.*, vol. 59, no. 1, pp. 96–102, 2021.

[8] ——, "Multimode high-altitude platform stations for next-generation wireless networks: Selection mechanism, benefits, and potential challenges," *IEEE Veh. Technol. Mag.*, vol. 18, no. 3, pp. 20–28, 2023.

[9] X. Qin *et al.*, "Joint optimization of resource allocation, phase shift, and UAV trajectory for energy-efficient RIS-assisted UAV-enabled MEC systems," *IEEE Trans. Green Commun. Network.*, vol. 7, no. 4, pp. 1778–1792, 2023.

[10] Z. Huang *et al.*, "Energy-efficient joint trajectory and reflecting design in IRS-enabled UAV edge computing," *IEEE IoT J.*, 2024.

[11] Z. Yao *et al.*, "Minimizing long-term energy consumption in RIS-assisted UAV-enabled MEC network," *IEEE IoT J.*, 2025.

[12] Z. Zhai *et al.*, "Energy-efficient UAV-mounted RIS assisted mobile edge computing," *IEEE Wireless Commun. Lett.*, vol. 11, no. 12, pp. 2507–2511, 2022.

[13] J. Shuai *et al.*, "Energy consumption minimization for UAV-mounted active RIS-assisted mobile edge computing," in *Proc. IEEE Int. Wrkshp. Radio Freq.Ant. Technol.*, 2024, pp. 516–521.

[14] Y. Li *et al.*, "Aerial reconfigurable intelligent surface-enabled URLLC UAV systems," *IEEE Access*, vol. 9, pp. 140 248–140 257, 2021.

[15] H. Ren *et al.*, "Energy minimization in RIS-assisted UAV-enabled wireless power transfer systems," *IEEE IoT J.*, vol. 10, no. 7, pp. 5794–5809, 2023.

[16] I. Rzig *et al.*, "UAV-assisted computation offloading in vehicular networks," in *Proc. IEEE Int. Perform. Comput. Commun. Conf. (IPCCC)*, 2023, pp. 236–241.

[17] Z.-Q. Luo *et al.*, "Semidefinite relaxation of quadratic optimization problems," *IEEE Sig. Process. Mag.*, vol. 27, no. 3, pp. 20–34, 2010.

[18] J. Kennedy and R. Eberhart, "Particle swarm optimization," in *Proc. Int. Conf. Neural Netw. (ICNN)*, vol. 4. IEEE, 1995, pp. 1942–1948.

[19] M. Hevesli *et al.*, "Multi-agent DRL for queue-aware task offloading in hierarchical MEC-enabled air-ground networks," *IEEE Trans. Cogn. Commun. Network.*, pp. 1–1, 2025.